Cell Calcium 47 (2010) 1–10

Contents lists available at ScienceDirect

Cell Calcium

journal homepage: www.elsevier.com/locate/ceca

Two novel 2-aminoethyl diphenylborinate (2-APB) analogues differentially activate and inhibit store-operated Ca^{2+} entry via STIM proteins

Jun-Ichi Goto[a,b,1], Akinobu Z. Suzuki[a,c,1], Shoichiro Ozaki[a], Nagisa Matsumoto[a], Takeshi Nakamura[c], Etsuko Ebisui[a], Andrea Fleig[b], Reinhold Penner[b], Katsuhiko Mikoshiba[a,c,d,*]

[a] Laboratory for Developmental Neurobiology, Brain Science Institute, RIKEN, 2-1 Hirosawa, Wako, Saitama 351-0198, Japan
[b] Center for Biomedical Research at the Queen's Medical Center and John A. Burns School of Medicine at the University of Hawaii, Honolulu, Hawaii, USA
[c] Division of Molecular Neurobiology, Department of Basic Medical Sciences, Institute of Medical Science, The University of Tokyo, 4-6-1 Shirokanedai, Minato-ku, Tokyo 108-8639, Japan
[d] Calcium Oscillation Project, International Cooperative Research Project-Solution Oriented Research for Science and Technology, Japan Science and Technology Agency, Saitama 332-0012, Japan

ARTICLE INFO

Article history:
Received 27 May 2009
Received in revised form 20 October 2009
Accepted 21 October 2009
Available online 27 November 2009

Keywords:
Store-operated calcium entry
CRAC
Calcium
STIM
Orai
CRACM
2-APB

ABSTRACT

Store-operated calcium entry (SOCE) or calcium release-activated calcium current (I_{CRAC}) is a critical pathway to replenish intracellular calcium stores, and plays indispensable roles in cellular functions such as antigen-induced T lymphocyte activation. Despite the importance of I_{CRAC} in cellular functions, lack of potent and specific inhibitor has limited the approaches to the function of I_{CRAC} in native cells. 2-Aminoethyl diphenylborinate (2-APB) is a widely used SOCE/I_{CRAC} inhibitor, while its effect is rather unspecific. In the attempt to develop more potent and selective compounds here we identified two structurally isomeric 2-APB analogues that are 100-fold more potent than 2-APB itself. One of the 2-APB analogues activates and inhibits endogenous SOCE depending on the concentration while the other only inhibits it. The 2-APB analogue inhibits store depletion-mediated STIM1 clustering as well as heterologously expressed CRAC current. Together with the observation that, unlike 2-APB, the analogue compounds failed to activate CRACM3/Orai3 current in the absence of STIM, our results suggest that inhibition and activation of SOCE/I_{CRAC} by the 2-APB analogues is mediated by STIM.

1. Introduction

Ca^{2+} is a universal second messenger that regulates contraction, secretion, plasticity, differentiation and other physiological functions in the cell [1]. In certain types of cells, receptor stimulation induces inositol 1,4,5-trisphosphate (IP_3)-induced Ca^{2+} release (referred as IICR) and thereby depletion of Ca^{2+} store activates store-operated calcium entry (referred as SOCE) [2]. Recent studies on SOCE revealed the mechanism by which the depleted internal store is replenished with calcium from the extracellular milieu. The endoplasmic reticulum-resident protein STIM [3–5] and pore-forming channel subunit CRACM (also known as Orai) [6–8] cooperatively constitute the I_{CRAC} channel [9]. The ablation of CRACM/Orai channels has been linked to human immunodeficiency [7] and to anaphylactic responses mediated by mast cells in mice [10], suggesting that the availability of pharmacological tools that allow the manipulation of CRAC may prove invaluable for the development of immunosuppressants or anti-allergic drugs.

Among the several CRAC channel inhibitors characterized so far [11–15] 2-aminoethyl diphenylborinate (2-APB) has been most commonly used and is a well-established CRAC inhibitor that, at lower concentrations, also acts as an activator of this current [16,17]. This prominent bimodal effect has been utilized to pharmacologically identify CRAC currents. However, 2-APB has proven to be rather unspecific, affecting diverse ion channel targets [18–21]. In an effort to improve the specificity of 2-APB towards IICR [22], we screened our library consisting of 600 2-APB analogues [23,24]. This resulted in the identification of two novel structural isomers that not only are significantly more potent CRAC inhibitors compared to 2-APB [25], but also reveal enhanced selectivity towards IICR. We also developed an efficient and convenient method to synthesize these compounds, which will be published elsewhere (Suzuki et al., in preparation).

Importantly, one of the isomers is a *bona-fide* CRAC inhibitor and does not lead to any CRAC activation at lower concentrations, while the other isomer retains a similar bimodal profile seen with 2-APB, albeit at higher potency. The only structural difference between

* Corresponding author at: Laboratory for Developmental Neurobiology, Brain Science Institute, RIKEN, 2-1 Hirosawa, Wako, Saitama 351-0198, Japan.
Tel.: +81 48 467 9745; fax: +81 48 467 9744.
E-mail address: mikosiba@brain.riken.jp (K. Mikoshiba).
[1] These authors contributed equally to this work.

0143-4160/$ – see front matter © 2009 Elsevier Ltd. All rights reserved.
doi:10.1016/j.ceca.2009.10.004

the two compounds is in the position of the bridge between two diphenylborinate (DPB) structures, suggesting that the activation of CRAC by that isomer critically depends on the accessibility of the compound to the channel proteins.

In addition to providing an important tool to elucidate mechanisms of CRAC channel activation and inhibition, these compounds may constitute novel candidates for therapeutic interventions.

2. Methods

2.1. Ca^{2+} imaging of DT40 cells

IP_3R-deficient DT40 cells were subjected to Ca^{2+} imaging as described previously [25]. Cells were treated with the drug of interest and the ER calcium store was depleted with 1 μM thapsigargin. Subsequently, 2 mM Ca^{2+} was added to the external solution to observe calcium entry. Detailed information is described in *Supplemental Data*.

2.2. Measurement of IP_3-induced Ca^{2+} release in cerebellar microsomes

Adult male ddY mice (8–10 weeks old; Nippon SLC, Japan) were deeply anaesthetized with ether, decapitated and the cerebella were quickly dissected. Isolation of microsomes from the cerebella and measurement of Ca^{2+} uptake and IICR were performed as described previously [26]. To test the effects of 2-APB analogues on IICR, they were added 2 min prior to IP_3 addition.

2.3. Ca^{2+} imaging using FDSS system

CHO-K1 cells, HeLa cells, SH-SY5Y cells and HEK293 cells were maintained in DMEM containing 10% FBS and plated in 96-well plate 2–3 days before the experiment. Before the recording, cells were washed three times with BSS(+), containing (in mM): 115 NaCl, 5.4 KCl, 2 $CaCl_2$, 1 $MgCl_2$, 10 glucose, and 20 HEPES (pH 7.4), and loaded with fura-2/AM for an hour, washed twice with BSS(−), which was identical to BSS(+) except that the Ca^{2+} was omitted and 0.5 mM EGTA was included. The cells were kept in BSS(−). Jurkat cells were maintained in RPMI1640 containing 10% FBS until the loading of fura-2. Before the measurement cells were washed with HBSS(+), containing (in mM): 137 NaCl, 5.4 KCl, 0.44 KH_2PO_4, 5.6 glucose, 0.34 Na_2HPO_4, 4.2 $NaHCO_3$, 1 $CaCl_2$ and 10 HEPES (pH 7.2), and loaded with fura-2/AM for an hour, washed with HBSS(−), which was identical to HBSS(+) except that the Ca^{2+} was omitted and 0.5 mM EGTA was included. To examine the effect of 2-APB analogues on SOCE in these cells we used FDSS-3000 system (Hamamatsu Photonics, Japan). After the addition of the drug of interest to the cells the ER calcium store was depleted with 1 μM thapsigargin. Subsequently, Ca^{2+} (2 mM in final concentration) was added in the external solutions and the peak height of the fluorescence ratio ($F_{340\,nm}/F_{380\,nm}$) was measured.

2.4. Electrophysiology

Patch-clamp recordings were performed as described previously [27]. Extracting the current amplitude at −80 mV from individual ramp current records assessed the low-resolution temporal development of currents. Standard external solution was as follows (in mM): 120 NaCl, 10 CsCl, 2.8 KCl, 2 $MgCl_2$, 10 $CaCl_2$, 10 TEA–Cl, 10 HEPES, and 10 glucose, pH was adjusted to 7.2 with NaOH, 300 mOsm. Each DPB compound was added to the standard external solution at certain concentrations with 0.1% (v/v) of final concentration of DMSO and applied through wide-tipped puffer pipettes. Internal solution was as follows (in mM): 120 Cs-glutamate, 20 Cs-BAPTA, 3 $MgCl_2$, 10 HEPES, and 0.02 inositol 1,4,5-trisphosphate (IP_3), pH was adjusted to 7.2 with CsOH, 300 mOsm. In the experiment of STIM2 expressing HEK293 cells, IP_3 was omitted from internal solution.

2.5. Clustering of STIM1 by store depletion

EGFP-STIM1-transfected HeLa cells were washed three times with BSS(+), then observed on an inverted microscope (IX81, Olympus) with 60× oil-immersion objective lens (PlanApoN, NA = 1.42, Olympus). Cells were treated with 1 μM of thapsigargin in BSS(−) for 10 min to test for the puncta formation. To examine the effect of compounds, cells were treated with 3 μM of DPB162-AE or DMSO (vehicle, for negative control) for 20 min after the thapsigargin treatment. Cells were examined for the reverse order experiment where the 10 min pre-incubation with 3 μM of DPB162-AE preceded the following 20 min of thapsigargin treatment (1 μM). Fluorescence signal was excited at 470–490 nm, selected with 510–550 nm emission filter and acquired with Cascade II EM-CCD camera (Photometrics) combined with CSU-X1 disc confocal unit (Yokogawa). Image acquisition and processing were done with MetaMorph software (Molecular Devices). Analysis of puncta was performed using wavelet analysis program written by Drs. Racine and Sibarita [28] to isolate clustered structures and threshold images were used to detect each punctate structure. Clusters less than 3 pixels of area (<0.2 μm^2) or of elongated shape ($4\pi \times$ area/(perimeter)^2 < 0.5, corresponds to the filamentous structures observed in the radial expression pattern of STIM1 before store depletion) were omitted from the analysis.

2.6. Western blotting

HeLa cells, SH-SY5Y cells, Jurkat cells and HEK293 cells were lysed with 1× SDS-PAGE sample buffer and the lysates were boiled and sonicated. Anti-STIM1 antibody (BD Transduction Laboratories, #610954) and anti-STIM2 antibody (Cell Signaling, #4917) were used in combination with the HRP-conjugated secondary antibody and the signals were developed by Immobilon Western (Millipore) and acquired using LAS-4000mini (Fujifilm). Data were analyzed by Multi Gauge Ver3.2 software (Fujifilm).

3. Results

3.1. Development of 2-APB analogues

To develop more potent SOCE inhibitors than 2-APB, we first established a library of over 600 chemical compounds derived from 2-APB [23,24]. Most compounds in the library include a 2-APB related boron-containing structure that seems to be an important element for blockade of SOCE [25]. These compounds were first screened with fluorescent Ca^{2+} imaging for their inhibitory effect on SOCE. They were also tested for their effect on IP_3-induced calcium release (IICR) since 2-APB attenuates IICR [22] in a similar concentration range of SOCE. To avoid this major side effect of 2-APB, we picked compounds that were highly active for SOCE inhibition while being less effective for IICR at the same concentration. This resulted in the identification of two structural isomers, DPB162-AE and DPB163-AE (where the DPB stands for diphenylborinate), which inhibited SOCE at very low concentration and yet had little effect on IICR in the same concentration range (Fig. 1). The isomers share basic structural characteristics: two 2-APB molecules are connected through a linker chain. The nature of the linker chain is an only difference between them.

The two compounds were further tested by establishing concentration–response curves in regards to their inhibitory effect on SOCE and IICR. To estimate the isomers' effect on SOCE, IP_3

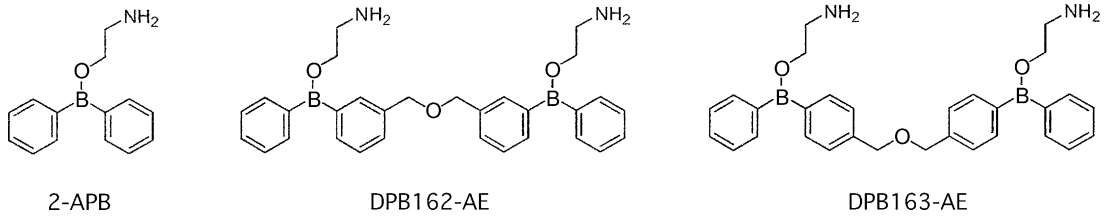

Fig. 1. Structure of 2-APB derived compounds.

receptor knock-out DT40 cells (which were targeted for all the three subtypes of IP_3 receptor [29]) were loaded with fura-2 AM, treated with each compound and the intracellular calcium store was depleted with thapsigargin in a calcium-free external solution. After store depletion, SOCE was measured by the addition of 2 mM Ca^{2+} to the external solution and assessed by the fura-2 signal measured in these cells. DPB162-AE showed a stronger inhibitory effect on SOCE than 2-APB (Fig. 2A). However, unlike 2-APB, DPB162-AE did not activate SOCE in DT40 cells at low concentrations (Fig. 2A). In contrast, DPB163-AE, similar to 2-APB, induced a profound activation of SOCE in DT40 cells, albeit at low concentrations (10 nM). This result indicates that the newly developed 2-APB analogues are more potent SOCE inhibitors than 2-APB, and the relatively minor difference in structure may determine the activation of SOCE.

3.2. Cell-type-specific effect of DPB compounds on SOCE

The molecular identity of Ca^{2+} influx channels stimulated by store depletion has long been awaited. The channel molecule CRACM/Orai and its stimulator STIM have recently been identified to constitute I_{CRAC} channel in mast cells and T lymphocytes [3–8,10,30–32]. Other molecules such as TRP channels are considered to be involved in store-operated Ca^{2+} influx in certain types of cells as well [33]. Since the responsible channel molecules for SOCE are not necessary the same, the effect of DPB compounds might be different among the certain types of cells.

To examine whether the two DPB compounds exert cell-type-specific responses, we additionally tested CHO-K1 and HeLa cells for SOCE using the Ca^{2+} imaging technique. DPB compounds blocked thapsigargin induced, store-operated Ca^{2+} influx in CHO-K1 cells (Fig. 2B and C). The most striking difference in the effect of DPB compounds between DT40 cells and CHO-K1 cells was their response to the low concentration of DPB163-AE. Unlike DT40 cells, SOCE in CHO-K1 cells was only inhibited but not activated by DPB163-AE (Fig. 2*C*). With an IC_{50} of 210 ± 20 nM and 45 ± 4 nM, respectively, the inhibitory efficacy of the DPB compounds seen in CHO-K1 cells was less than that of DT40 cells (Fig. 2D). In HeLa cells, DPB163-AE activated SOCE at low concentrations between 60 and 200 nM (Fig. 2F), but the relative amplitude of activation was not as much as that of DT40 cells. The inhibitory efficacy of both compounds were less in HeLa cells than in CHO-K1 cells, and the residual Ca^{2+} elevation resistant to higher concentrations of compounds seemed to be larger in HeLa cells, which was negligible in CHO-K1 cells (Fig. 2G). These results suggest that different types of cells may contain different SOCE-constituting molecules with distinct responses to antagonists.

3.3. Each CRACM/Orai channel subtype responds differently to DPB compounds

The variability in the effects of DPB compounds among each cell type may reflect the differences in the molecular composition of store-operated calcium channels in each cell line. I_{CRAC} is a major pathway of the store-operated calcium entry (SOCE) in mast cells and T lymphocytes and requires two proteins, STIM and CRACM (also known as Orai). There are reportedly two subtypes of STIM proteins (STIM1 and STIM2) and three of CRACM/Orai (CRACM1/Orai1–3), each of them with different characteristic properties [4,5,34,35]. To address the effect of the compounds on different subtypes of CRACM/Orai channels we performed patch-clamp recording using a heterologous expression system of HEK293 cells and evaluated subtype-specificity of the responses to DPB compounds. HEK293 cells stably expressing STIM1 were transiently transfected with CRACM1/Orai1 and the IP_3-sensitive calcium store was depleted by adding 20 μM IP_3 to the internal solution. After the full activation of I_{CRAC}, the test compound was applied to evaluate its effect. Both DPB162-AE and DPB163-AE almost completely blocked STIM1 and CRACM1/Orai1-mediated I_{CRAC} within 3 min of compound application at 1 μM (Fig. 3A and C). The current–voltage (I/V) curves show that the current–voltage relationship was not altered after the application ("voltage-independent block", Fig. 3B and D) for both compounds. With IC_{50} values of 86 ± 21 nM for DPB162-AE and 170 ± 68 nM for DPB163-AE, the dose–response curves had a similar range of inhibitory efficacy of I_{CRAC} as observed for SOCE in CHO-K1 cells (Fig. 3E).

I_{CRAC} has been characterized by its unique response to 2-APB [12]. It is activated by low concentration (~5 μM) of 2-APB and blocked at higher concentration (>30 μM). The observation that low concentration of DPB163-AE, but not DPB162-AE activated I_{CRAC} in DT40 cells and HeLa cells suggests that the molecular composition of the CRAC channel may play a key role in the determination of activation and inhibition of this current. Since the dose–response curve for DPB163-AE on STIM1 and CRACM1/Orai1 overexpressing HEK293 cells did not show a clear activation of I_{CRAC} (Fig. 3*E*), we next examined other CRACM/Orai channels for an effect mediated by the two DPB compounds.

CRACM2/Orai2 was transiently expressed in STIM1 expressing HEK293 cells and the effect of the compounds was examined as described for CRACM1/Orai1 above. CRACM2/Orai2-mediated I_{CRAC} was sensitive to the DPB compounds, however the block was less pronounced and the inhibitory effect reached a plateau (Fig. 4A and C). Similar to CRACM1/Orai1, the mode of blockade was voltage-independent for both compounds (Fig. 4B and D). The partial inhibition of CRACM2/Orai2 is also observed for 2-APB, suggesting that the DPB compounds and 2-APB share a common underlying mechanism by which the current is inhibited [27]. However, these results did not explain how endogenous SOCE is activated by DPB163-AE, since there was no activation of CRACM2/Orai2 current by either of the two compounds.

The third member of CRACM/Orai channels, CRACM3/Orai3, is known to show the unique response to 2-APB: this channel is only activated by 2-APB and is never blocked [27,36–38]. To elucidate whether CRACM3/Orai3 can be activated by DPB compounds we tested STIM1-CRACM3/Orai3 expressing HEK293 cells. Similar to 2-APB, both DPB162-AE and DPB163-AE facilitated CRACM3/Orai3 currents at lower concentrations (~100 nM), however, at higher concentrations (>300 nM) they transiently activated and subsequently deactivated I_{CRAC} (Fig. 4E–H). Both compounds did not completely inhibit the current, even at a 10 μM concentration. This

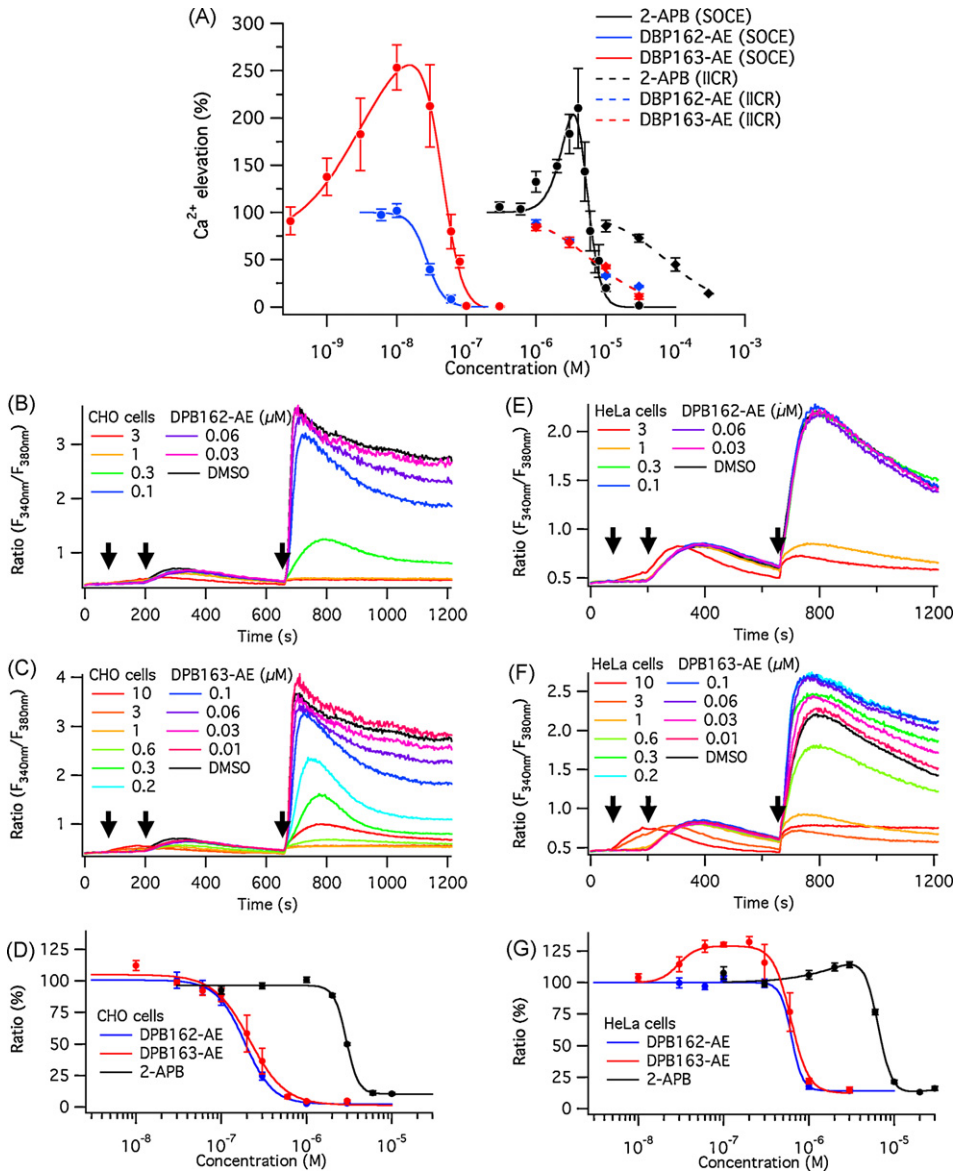

Fig. 2. 2-APB-derived compounds inhibit SOCE. (A) Average fluorescence ratio ($F_{340\,nm}/F_{380\,nm}$) change shown for both the SOCE measurement (circles and solid lines), and the IICR measurement (diamonds and dashed lines). The curve fits show the estimated dose–responses for each compound. 2-APB has conspicuous activation and inhibition phases within a narrow range of concentrations (solid black line). DPB162-AE (solid blue line) does not activate SOCE at low concentrations. The activation phase induced by DPB163-AE is similar to that of 2-APB but shifted to the left (solid red line). Both DPB compounds inhibit SOCE at much lower concentration than 2-APB. Both DPB162-AE and DPB163-AE (dashed blue and red lines, respectively) are less effective in blocking IICR compared to SOCE, but similar to 2-APB (dashed black line). IC_{50} for SOCE is 4.8 ± 0.6 μM, 27 ± 2 nM and 42 ± 3 nM for 2-APB, DPB162-AE and DPB163-AE, respectively (Hill coefficients of 4.0, 3.5 and 2.7). EC_{50} for the activation phase of SOCE is 3.6 ± 0.6 μM and 5.9 ± 0.9 nM for 2-APB and DPB163-AE, respectively (Hill coefficients of 3.2 and 1.1). IC_{50} for IICR is 73 ± 8 μM, 6.3 ± 0.9 μM and 6.3 ± 0.9 μM for 2-APB, DPB162-AE and DPB163-AE, respectively (Hill coefficients of 1.1, 1.0 and 1.0). (B–D) Shown are representative data from Ca^{2+} imaging experiments in CHO cells performed with DPB162-AE and DPB163-AE (B and C, respectively). Neither compound reveals an evident activation phase in its dose–response curve (D). IC_{50} for 2-APB, DPB162-AE and DPB163-AE in CHO cells is 2.9 ± 0.1 μM, 190 ± 6 nM and 210 ± 20 nM with Hill coefficients of 6.1, 2.6 and 2.1, respectively. (E–G) Depicted are representative data from Ca^{2+} imaging experiments in HeLa cells. Unlike observed in CHO cells, DPB162-AE (E) blocks but does not activate SOCE. In contrast, DPB163-AE (F) activates SOCE at low concentrations, similar to DT40 cells. The residual part of the calcium entry, which is not blocked by higher doses of compounds, seems to be larger in HeLa cells than in CHO or DT40 cells. Dose–response curves of HeLa cells for DPB compounds show a similar range of IC_{50} when compared to CHO cells, while at low concentration of DPB163-AE an activation phase can be observed similar to DT40 cells. IC_{50} for 2-APB, DPB162-AE and DPB163-AE in HeLa cells is 6.5 ± 0.3 μM, 620 ± 210 nM and 620 ± 39 nM with Hill coefficients of 5.2, 6.7 and 4.2, respectively. EC_{50} for the activation phase of SOCE is 3.3 ± 3.5 μM and 30 ± 6.8 nM for 2-APB and DPB163-AE with Hill coefficients of 1.3 and 4.1, respectively. Arrows in B, C, E and F indicate the timing (left to right) of compound application, addition of 1 μM thapsigargin and addition of 2 mM external Ca^{2+}. All the data points in A, D and G are given as mean ± SEM. (For interpretation of the references to color in this figure legend, the reader is referred to the web version of the article.)

suggests that I_{CRAC} activation induced by these compounds target CRACM3/Orai3 at low concentrations.

The differential responses of each of the CRACM/Orai subtype to the two antagonists suggest that the compound sensitivity of each cell line can be explained by the specific CRACM/Orai subtypes expression in the cells. Almost complete blockade of SOCE by the compounds and no apparent activation in CHO-K1 cells suggests that the major part of the SOCE in CHO-K1 cells may be mediated by CRACM1/Orai1. In HeLa cells, both compounds did not completely block the SOCE, indicating CRACM2/Orai2 and/or CRACM3/Orai3 may contributes to the SOCE or there might be another channel involved which is resistant to these compounds.

To further investigate the effect of the boron-containing compounds we next tested the STIM2 and CRACM1/Orai1 over-

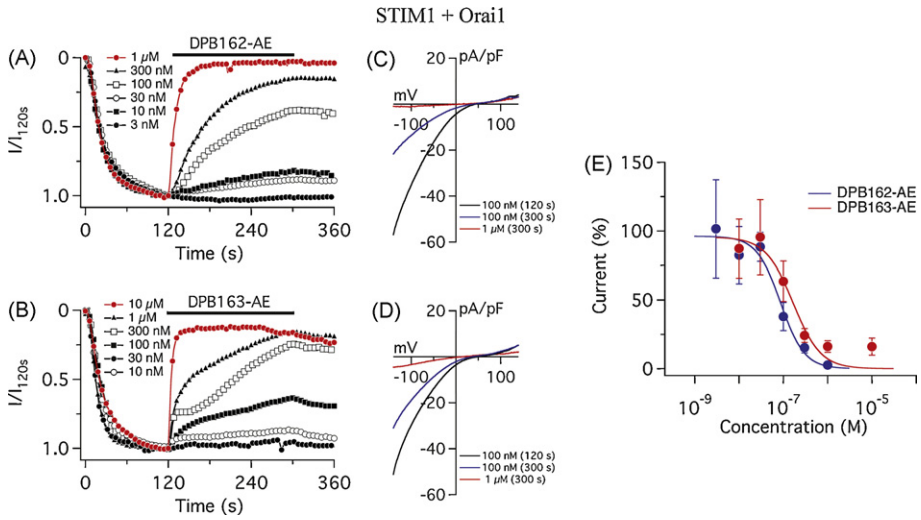

Fig. 3. Differential effects of 2-APB analogs in dependence of CRACM/Orai subtype: CRACM1/Orai1. (A) Average CRAC current densities assessed at −80 mV in STIM1 and CRACM1/Orai1 expressing HEK293 cells. I_{CRAC} was induced by 20 μM IP_3 in the internal solution. DPB162-AE was applied 120 s after whole-cell break-in as indicated by the black bar. 1 μM DPB162-AE almost completely blocks I_{CRAC} (red trace, $n = 4$). At 300 nM ($n = 5$) to 100 nM ($n = 6$), it blocks I_{CRAC} more than a half after the 3 min of application. Lower concentrations, 30 nM ($n = 8$), 10 nM ($n = 3$) and 3 nM ($n = 3$) have less effect on I_{CRAC}. (*B*) Average current–voltage (I/V) relationships of I_{CRAC} of representative concentrations of DPB162-AE shown in (A). Data represent I_{CRAC} before (at 120 s) and after (at 300 s) application of 100 nM DPB162-AE and the current after application of 1 μM. (C) Average CRAC current densities at −80 mV in STIM1 and CRACM1/Orai1 expressing HEK293 cells treated with DPB163-AE at the concentration of 10 μM ($n = 3$), 1 μM ($n = 8$), 300 nM ($n = 9$), 100 nM ($n = 10$), 30 nM ($n = 5$) and 10 nM ($n = 6$). (D) Average current–voltage relationships of I_{CRAC} of representative data shown in (C). (E) Dose–response curves of STIM1-CRACM1/Orai1 based I_{CRAC} for DPB162-AE and DPB163-AE (in blue and red, respectively). Each data point shows the measured average current density at 300 s normalized by the current assessed before the application (at 120 s). No apparent activation was observed for both compounds. Error bars indicate SEM. (For interpretation of the references to color in this figure legend, the reader is referred to the web version of the article.)

expressing HEK293 cells. Since STIM2-mediated CRAC current is activated by 2-APB as well as dialysis of cytoplasm during the whole-cell patch-clamp recording without any store depletion [39], we applied the compounds before the dialysis-evoked current developed. Both DPB162-AE and DPB163-AE activated I_{CRAC} at 1 μM and 300 nM, but the amount of activation appeared to be larger for DPB163-AE than DPB162-AE (Fig. 5A and B). In addition, 100 nM of DPB163-AE appeared to slightly activate the early phase of I_{CRAC} while DPB162-AE had no significant effect of activation on STIM2-CRACM1/Orai1-mediated current, and rather blocked the induction of the current (Fig. 5C). This result indicates that STIM2 might be responsible for the differential effect on SOCE seen with DPB162-AE and DPB163-AE in some cell lines (Fig. 2).

The above results with STIM and CRACM/Orai overexpressing cells show both molecules contribute to the characteristics of the responses of I_{CRAC} to the boron-containing compounds. To elucidate the effect of the compounds on CRACM/Orai channels directly, we tested HEK293 cells expressing each CRACM/Orai molecule alone without exogenous STIM. Here, DPB163-AE appeared to slightly activate I_{CRAC}-like current in some CRACM1/Orai1 expressing cells (Fig. S1B). This effect, however, was more ambiguous for CRACM2/Orai2 or CRACM3/Orai3 expressing cells, which did not show significant responses (Fig. S1D and F). DPB162-AE did not cause clear activation of I_{CRAC} for all three subtypes of CRACM/Orai channels (Fig. S1A, C and E). These results indicate that the DPB-induced facilitation of CRACM3/Orai3 is most likely to be mediated by a STIM-dependent mechanism, in contrast to 2-APB itself, which is able to activate CRACM3/Orai3 independent of STIM [27,36–38].

3.4. DPB compounds inhibit the clustering of STIM1 upon the store depletion

Since the activation of CRACM/Orai channel by STIM1 is triggered by the translocation and the clustering of STIM1 upon store depletion [4,40–43], we hypothesized that the boron-containing compounds also interfere with the clustering of STIM1. To elucidate the effect of the DPB compounds, HeLa cells expressing STIM1 fused with EGFP at N-terminus (EGFP-STIM1) were treated with thapsigargin to deplete calcium stores. STIM1 proteins were relatively sparsely distributed in a radial manner at rest, while they formed dense puncta upon thapsigargin-mediated store depletion. EGFP-STIM1 clusters dispersed after the treatment with 3 μM of DPB162-AE (Fig. 6A). In addition, pre-incubation of the cells with DPB162-AE prevented STIM1 puncta formation (Fig. 6B), indicating that DPB162-AE may act on STIM1 to block I_{CRAC}. Analysis of averaged area of clustered fluorescence signals revealed increased clusters upon store depletion almost reversed by DPB162-AE, while pre-incubation of cells with DPB162-AE almost completely blocked the thapsigargin-induced enlargement of punctate signals (Fig. 6C).

3.5. Expression level of STIM proteins conforms to differential activation of SOCE

To further dissect the role of STIM proteins in the effect of the compounds on SOCE, we have tested endogenous SOCE in some types of cells and also examined the expression level of STIM1 and STIM2 for those cells (Fig. 7). HeLa cells and HEK293 cells showed moderate activation of SOCE by low concentration of DPB163-AE (132.3 ± 4.1% at 0.2 μM and 120.4 ± 2.2% at 0.1 μM, respectively) while SH-SY5Y cells exhibited much higher level of activation (158.5 ± 3.0% at 0.1 μM). Compared with these cells, little amount of activation of SOCE was observed in Jurkat T cells (106.4 ± 4.5% at 0.2 μM, Fig. 7A). We did not observe significant level of activation in SOCE by DPB162-AE for any of these cells. Western blot analysis was performed for these cells to assess the expression level of STIM1 and STIM2 (Fig. 7B) and relative expression amount of STIM2 against STIM1 was estimated. SH-SY5Y cells exhibited relatively high expression level of STIM2 while other cells showed similar ratio of STIM2/STIM1 expression level. This expression pattern suggests that the relatively high level of STIM2 expression may contribute to the higher activation of SOCE by DPB163-AE in SH-SY5Y cells.

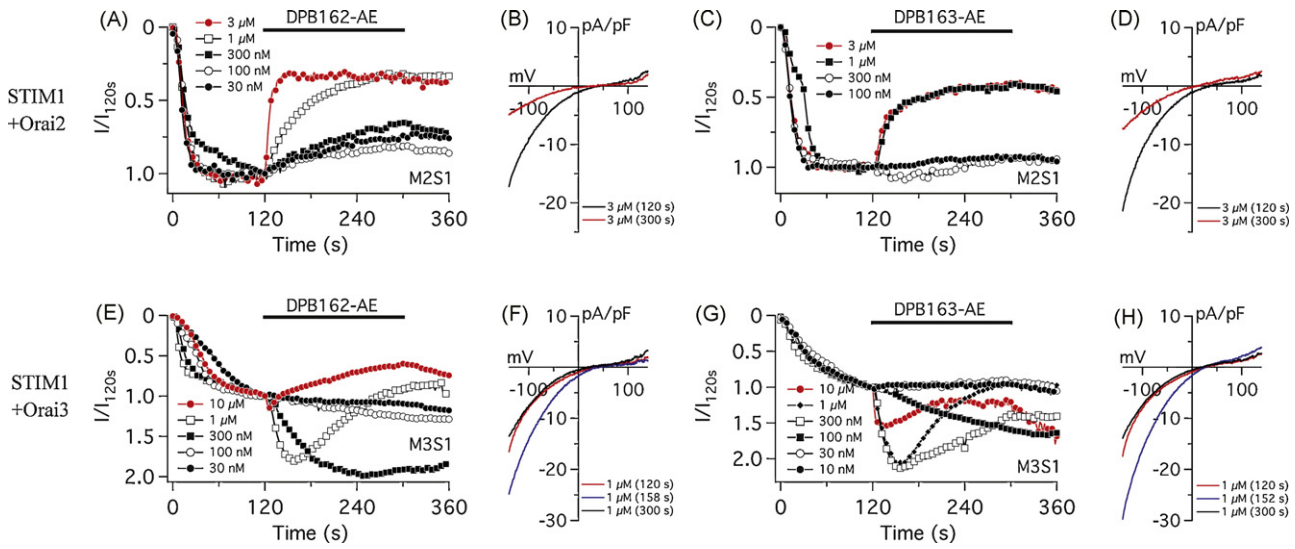

Fig. 4. Differential effects of 2-APB analogs on CRACM2/Orai2 and CRACM3/Orai3. (A and C) Average CRAC current densities in STIM1 and CRACM2/Orai2 expressing HEK293 cells. DPB162-AE (A) or DPB163-AE (C) was applied 120 s after whole-cell establishment. Each trace represents 3 μM ($n = 3$), 1 μM ($n = 3$), 300 nM ($n = 4$), 100 nM ($n = 4$) and 30 nM ($n = 3$) of DPB162-AE in (A), and represents 3 μM ($n = 3$), 1 μM ($n = 3$), 300 nM ($n = 5$) and 100 nM ($n = 3$) of DPB163-AE in (C). (B) Average I/V relationships of I_{CRAC} of representative concentrations of DPB162-AE shown in (F). Data represent I_{CRAC} before (at 120 s) and after (at 300 s) the application of 3 μM DPB162-AE. (D) Average I/V relationships before and after the application of DPB163-AE. (E and G) Average CRAC current densities at −80 mV in STIM1 and CRACM3/Orai3 expressing HEK293 cells. Initial activation of I_{CRAC} and application of compound were performed same way as in Fig. 3A and C. Compound application induces transient or prolonged activation of CRACM3/Orai3 current depending concentration. Each trace represents 10 μM ($n = 4$), 1 μM ($n = 3$), 300 nM ($n = 5$), 100 nM ($n = 4$) or 30 nM ($n = 4$) of DPB162-AE in (E), and represents 10 μM ($n = 3$), 1 μM ($n = 6$), 300 nM ($n = 5$), 100 nM ($n = 4$), 30 nM ($n = 4$) or 10 nM ($n = 3$) of DPB163-AE in (G). (F) Average I/V relationships of I_{CRAC} of representative concentrations of DPB162-AE shown in (E). Data represent I_{CRAC} before (at 120 s), during (at 158 s) and at the end (at 300 s) of the application of 1 μM DPB162-AE. (H) Average I/V relationships of CRAC currents of representative concentrations of DPB163-AE shown in (G). Data represent CRAC currents before (at 120 s), during (at 152 s) and at the end (at 300 s) of the application of 1 μM DPB163-AE.

4. Discussion

Store-operated calcium entry is one of the most important pathways for calcium signaling in non-excitable cells yet the identification of the current has been relatively difficult because of the apparent heterogeneity of responsible channels, very small conductance of the well-characterized current I_{CRAC} and, until recently, lack of knowledge about the molecular identity of the SOC channels. 2-APB has been an important pharmacological tool in the field of SOCE/I_{CRAC}, due to its unique characteristic of activating SOCE/I_{CRAC} at low concentrations (~5 μM) and the inhibitory effect seen at higher concentrations (≥30 μM) [16,17]. To obtain more potent as well as SOCE-selective inhibitors, we developed novel 2-APB derivatives that preferentially inhibit SOCE while only marginally affecting IP_3 receptors. Although these compounds are structurally related isomers, they had very distinct effects on SOCE. While DPB163-AE revealed a bimodal effect on SOCE in analogy to 2-APB, DPB162-AE accomplished inhibition only (Fig. 2A). Distinct mechanisms for activation and inhibition of I_{CRAC} by 2-APB have been proposed to explain its bimodal effect [27], suggesting that the difference in activation of SOCE between two DPB compounds might originate from their differential effects on CRACM/Orai proteins. As these compounds are similar in structure to 2-APB, we assumed that their mechanism of action on I_{CRAC} might be similar as well. However, DPB compounds did not activate CRACM3/Orai3 without STIM1 (Fig. S1E and F), apparently indicating poor accessibility of these compounds to the pore of CRACM3/Orai3. As 2-APB has been suggested to affect the pore region of CRACM3/Orai3 to gate independent of STIM [27,36,37], this difference might be caused by the larger size of DPB compounds, which may prevent them from accessing the pore of CRAC channels. Reversal potential of CRACM3/Orai3 current in STIM1 background was not significantly affected by DPB compounds (32.5 ± 4.5 mV and 34.8 ± 4.3 mV, before and after the application of DPB162-AE, respectively, $n = 9$; 36.0 ± 7.4 mV and 38.1 ± 8.6 mV, before and after the application of DPB163-AE, respectively, $n = 11$), also suggesting that these compounds activate CRACM3/Orai3 current in a different manner from 2-APB. Together with the results that DPB162-AE reversed the

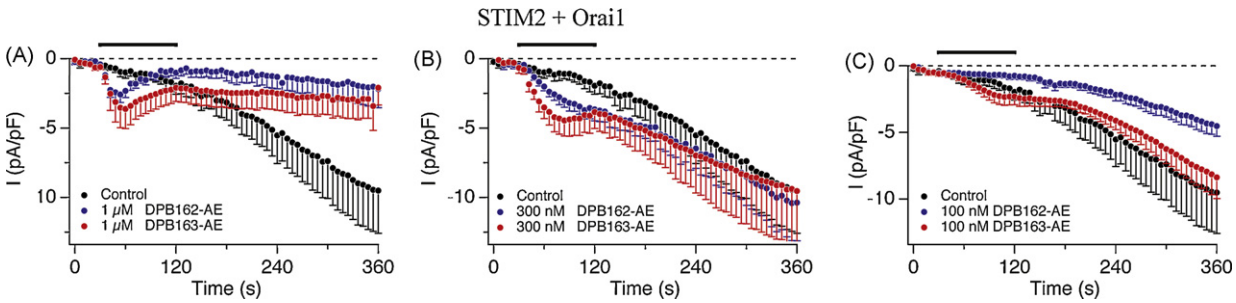

Fig. 5. DPBs activate STIM2-mediated CRAC currents independent of store depletion. (A–C) Average CRAC current densities at −80 mV in STIM2 and CRACM1/Orai1 expressing HEK293 cells. I_{CRAC} was activated by application of DPB162-AE or DPB163-AE in the absence of IP_3 in the internal solution. Application started before the dialysis-activated STIM2 current was induced. Each trace represents 1 μM ($n = 6$), 300 nM ($n = 4$) or 100 nM ($n = 6$) of DPB162-AE, and 1 μM ($n = 3$), 300 nM ($n = 4$) or 100 nM ($n = 7$) of DPB163-AE, together with the non-applied negative control trace ($n = 7$).

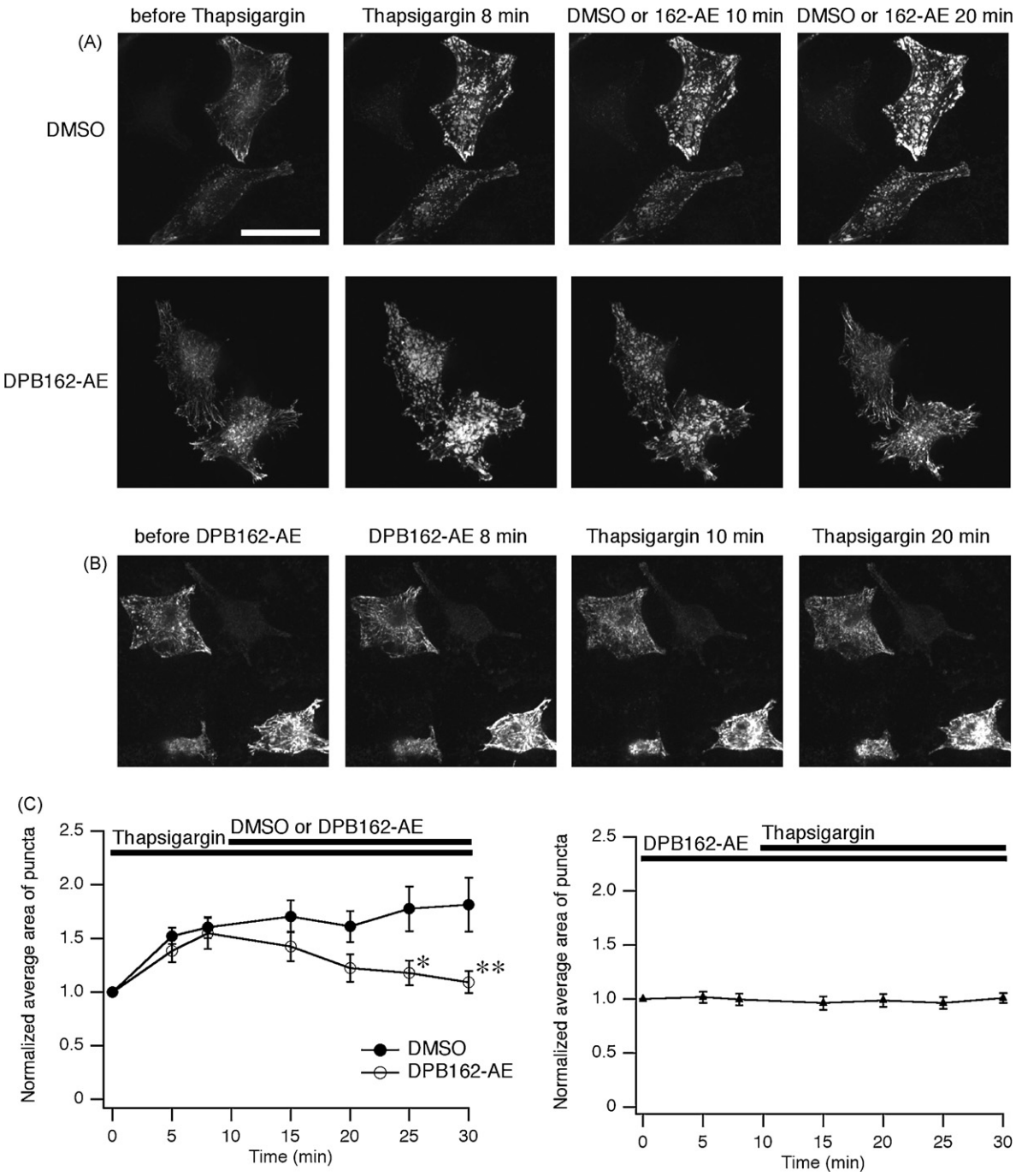

Fig. 6. DPB162-AE inhibits thapsigargin-induced puncta formation of STIM1. (A) HeLa cells were transfected with EGFP-STIM1 to visualize their localization. In the resting state STIM1 proteins distribute in a radial and sparse manner throughout the cell ("before Thapsigargin"). Cells were treated with 1 μM of thapsigargin for 10 min then 3 μM of DPB162-AE or DMSO (for negative control) was added. After 8 min treatment with thapsigargin causes translocation of STIM1 into puncta ("Thapsigargin 8 min"). Following application of DMSO did not interfere with cluster formation (upper panels). Clustered EGFP-STIM1 dispersed upon following application of DPB162-AE (lower panels). (B) Pre-incubation with 3 μM of DPB162-AE for 10 min prevents the puncta formation induced by thapsigargin treatment. Twenty minutes of thapsigargin treatment (1 μM) failed to induce distinct clustered structures as observed in (A) ("Thapsigargin 20 min"). (C) Fluorescence puncta were identified and analyzed for the average area. Store depletion by thapsigargin treatment increased average area of puncta while 20 min incubation with 3 μM of DPB162-AE reversed the clustering almost to the baseline level (left panel). The effect of DPB162-AE on the average area of puncta was significant compared with DMSO negative control ($^{*}P < 0.02$ at 15 min after DPB162-AE applied, $^{**}P < 0.001$ at 20 min after DPB162-AE applied, *t*-test. $n = 5$ and 9 for DMSO and DPB162-AE, respectively). In contrast, HeLa cells pretreated with DPB162-AE did not show clear increase in average area of clusters (right panel, $n = 17$). Data points represent mean ± SEM. Scale bar: 50 μm.

STIM1 puncta formed upon store depletion and prevented the formation of puncta by pre-incubation (Fig. 6), DPB162-AE seems to behave more like a STIM inhibitor than a CRAC channel pore modulator.

On the other hand, DPB163-AE activated SOCE at low concentration, which could be explained by the differential effect of these compounds on STIM proteins. Recent study by Wang et al. [44] revealed that 2-APB activates CRAC current by facilitating the coupling of the C-terminal region of STIM with CRACM/Orai channel. Given the DPB compounds share the common mechanism of action on STIM proteins with 2-APB, stronger coupling of STIM with CRACM/Orai by DPB163-AE than DPB162-AE might cause the

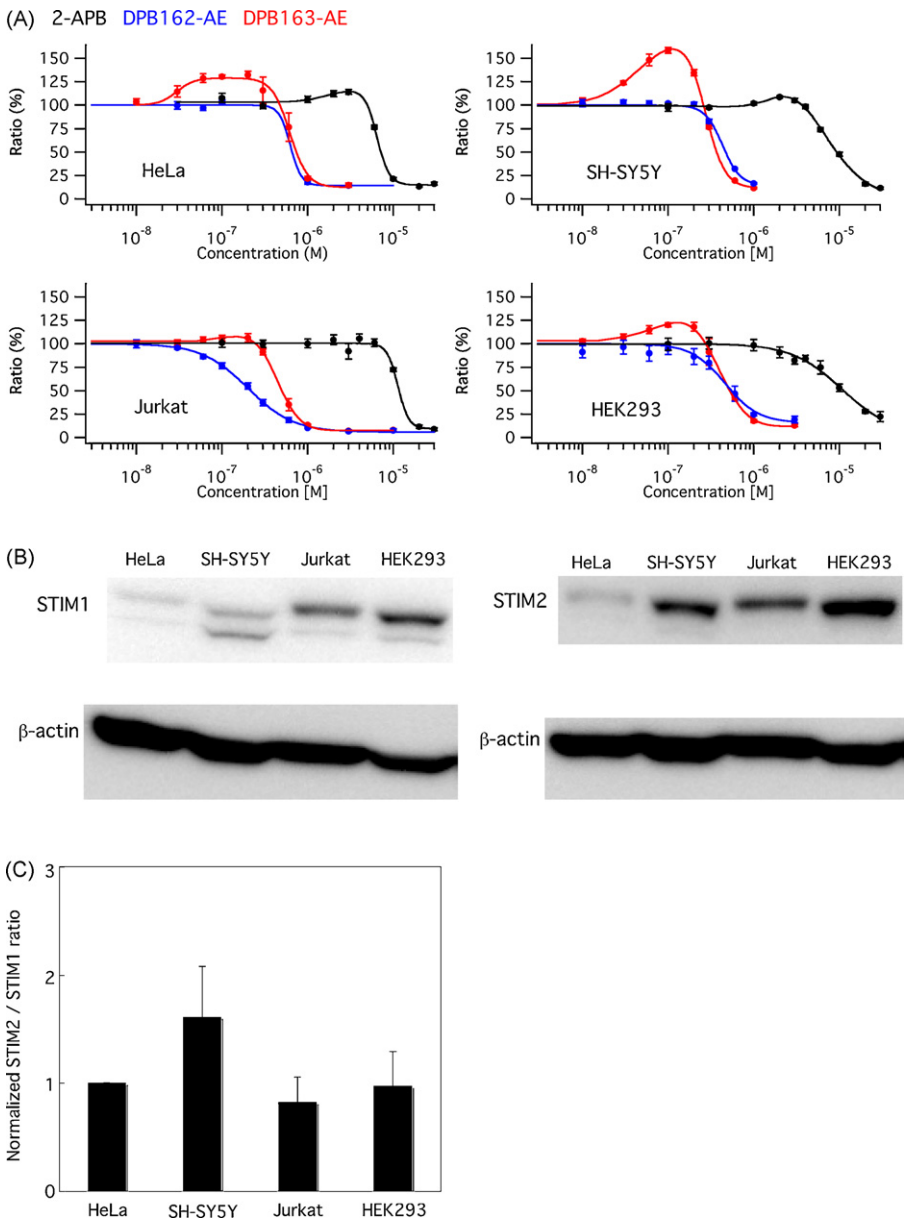

Fig. 7. Differential activation of SOCE by DPB163-AE and expression level of STIM proteins in human cell lines. (A) HeLa, SH-SY5Y, Jurkat and HEK293 cells were examined for dose–response of 2-APB, DPB162-AE and DPB163-AE. SOCE was differentially activated by low concentration of DPB163-AE among different cell types. (B and C) Expression level of STIM1 and STIM2 was determined by western blot and relative expression level of STIM2 against STIM1 was normalized with the value obtained from HeLa cells (1.61 ± 0.47, 0.82 ± 0.24, 0.98 ± 0.32 for SH-SY5Y, Jurkat and HEK293, respectively, $n = 4$). Data were shown in mean ± SEM.

differential effect on SOCE. The important notion is that 2-APB facilitate the rapid association between C-terminal coiled-coil domain of STIM and CRACM/Orai, then activate CRAC current in a distinct way from constitutive Ca^{2+} entry [44]. DPB162-AE treatment induced very tiny puncta of EGFP-STIM1 (data not shown) like as observed for 2-APB, suggesting that the modulation of CRAC by these compounds may include both of the association and the dissociation of the STIM-CRACM/Orai complex. Further analysis with mutated STIM and CRACM/Orai proteins may provide information about both DPB-mediated activation and inhibition mechanisms of I_{CRAC} and the structural basis of their regulation of the CRAC channel.

In addition to the differential effects between two DPB compounds, DPB163-AE showed the differential activation of SOCE among different types of cells (Figs. 2 and 7). Notably, DPB163-AE induced activation of SOCE in DT40 cells, HeLa cells, SH-SY5Y cells and HEK293 cells, however, little or almost no activation was observed in CHO cells and Jurkat cells. Since only the molecular combination of CRACM3/Orai3-STIM1 and STIM2-CRACM/Orai were facilitated by DPBs (Figs. 4 and 5), this difference could be explained by the differential contribution of each subtype of CRACM/Orai and STIM to SOCE in these cell types. There is no CRACM3/Orai3 gene found in chick genome [44] may suggest that STIM2 is responsible for this activation in DT40 cells. We have examined the expression of STIM1 and STIM2 in human cell lines and the relatively high expression level of STIM2 seems to coincide with high level of activation of SOCE by DPB163-AE in SH-SY5Y cells (Fig. 7). Our results do not necessary exclude the possible contribution of CRACM3/Orai3 or other types of channels, and the relative contribution of STIM2 and CRACM3/Orai3 (or other types of channels) to the generation of differential activation of SOCE will be interesting to learn in future studies.

In summary, we established highly potent SOCE/I_{CRAC}

[42] J. Liou, M. Fivaz, T. Inoue, T. Meyer, Live-cell imaging reveals sequential oligomerization and local plasma membrane targeting of stromal interaction molecule 1 after Ca^{2+} store depletion, Proc. Natl. Acad. Sci. U.S.A. 104 (2007) 9301–9306.
[43] Y. Baba, K. Hayashi, Y. Fujii, A. Mizushima, H. Watarai, M. Wakamori, T. Numaga, Y. Mori, M. Iino, M. Hikida, T. Kurosaki, Coupling of STIM1 to store-operated Ca^{2+} entry through its constitutive and inducible movement in the endoplasmic reticulum, Proc. Natl. Acad. Sci. U.S.A. 103 (2006) 16704–16709.
[44] Y. Wang, X. Deng, Y. Zhou, E. Hendron, S. Mancarella, M.F. Ritchie, X.D. Tang,